

1 Towards Autonomy: A Recommender System for the
2 Determination of Trim and Flight Parameters for
3 Seaglidern

4 Enrico Anderlini^{a,*}, Catherine Harris^b, Alexander B. Phillips^b,
5 Alvaro Lorenzo Lopez^b, Mun Woo^c, Giles Thomas^a

6 ^a*Department of Mechanical Engineering, Roberts Building, University College London,*
7 *Torrington Place, London, WC1E 7JE, UK*

8 ^b*Marine Autonomous and Robotic Systems, National Oceanography Centre, European*
9 *Way, Southampton, SO14 3ZH, UK*

10 ^c*Australian National Facility for Ocean Gliders, University of Western Australia, 35*
11 *Stirling Highway, Crawley, WA 6009, Australia*

12 **Abstract**

Currently, pilots maximise the performance of Seaglider underwater gliders by manually selecting their set-up parameters. Building on existing procedures based on the assumption of steady-state motions, a recommender system for the trim and flight parameters has been developed to aid trainee pilots and enable round-the-clock operations. The system has been validated with data from 12 missions run in waters off the United Kingdom and Australia, representative of a range of oceanographic conditions. **The recommended trim parameters present a maximum difference of 14% from the values selected by the pilots, whereas pilots are found not to change the flight parameters.** Additionally, suggestions are made to improve operational practices to further improve the accuracy of the recommender system. As a result, the developed system is expected to greatly help trainee pilots achieve expertise in a much smaller time frame than standard practice. Additionally, thanks to its high precision, the recommender system can be used to autonomously select the trim and flight parameters of Seaglidern for night operations in the future.

13 *Keywords:* Autonomous underwater vehicle (AUV), underwater glider,
14 system identification, recommender system

*Principal corresponding author

Email address: E.Anderlini@ucl.ac.uk (Enrico Anderlini)
Preprint submitted to Ocean Engineering

August 15, 2019

15 1. Introduction

16 Underwater gliders (UGs) represent a type of autonomous underwater
17 vehicles (AUVs) whose vertical motion is obtained through changes in their
18 buoyancy and is converted into horizontal motion through wings (Rudnick,
19 2016). As a result, they move in a characteristic vertical zigzag pattern or
20 profile. Although they move at slow velocities, their propulsion system, which
21 consists only of a variable buoyancy device (VBD), roll and pitch control
22 mechanisms and sometimes a rudder, is very efficient and as a result UGs
23 may be deployed for months in an area of operation. Therefore, since the first
24 conceptual description in the visionary article by Stommel (1989), UGs have
25 now become a fundamental tool for the study of the oceans (Rudnick, 2016).
26 Not only are they used to study large-scale effects, e.g. boundary currents
27 and the regional effects of climate variability, but also smaller scale effects
28 like mesoscale and submesoscale features such as fronts and eddies (Rudnick,
29 2016). Thorough reviews of UG technology with a focus to oceanographic
30 applications may be found in Davis et al. (2003), Wood (2009) and Rudnick
31 (2016).

32 The National Oceanography Centre (NOC) in the UK operates a fleet
33 of UGs for the study of the oceans, collaborating with the Scottish Asso-
34 ciation of Marine Sciences and the University of East Anglia. As part of
35 the Oceanids project funded by the Industrial Strategy Challenge Fund¹, the
36 NOC is developing a new command-and-control system for efficient marine
37 autonomous systems fleet management. The aim of the system is to facilitate
38 the operation of the ever-increasing fleet of AUVs. As part of this work, a
39 recommender system for the selection of the trim and flight parameters of
40 UGs is highly desired.

41 A recommender system provides users with suggestions on the products,
42 services and information that best meet their needs (Aggarwal, 2016). Nowa-
43 days, the most familiar types of recommender systems are based on machine
44 learning and can be found on internet platforms for the streaming of music
45 and videos or the selling of products. Nevertheless, recommender systems are
46 also found in the aerospace industry to help pilots with decision-making tasks
47 for increased safety, as shown for instance by Dao et al. (2015), Bouzekri et al.
48 (2017) and even the patent by Kim et al. (2017). The role of pilots of UGs
49 is different from those of commercial aircraft: UGs are autonomous vehicles

¹<https://noc.ac.uk/projects/oceanids>

50 that can perform a specified mission independently. However, the pilots need
51 to correctly determine the UG's trim and dynamic parameters and send them
52 to the UG remotely by satellite communication so that they may be imple-
53 mented onto the on-board controller (IRobot, 2012). Therefore, similarly to
54 the aerospace industry, the recommender system would support rather than
55 automate the operators' decision making. Thus, the recommender system
56 would return recommended values to the pilots within the fleet management
57 software. However, pilots would be still able to overwrite the system so that it
58 would not represent fully autonomous operation. Initially, the recommender
59 system may help trainee pilots to determine the correct set-up of UGs. Once
60 the system has been proven to be effective and robust, it may be used during
61 night time and to help expert pilots track the operation of multiple UGs.

62 This article focuses on Seaglidors, a type of UG developed originally by
63 the University of Washington and first described in Eriksen et al. (2001).
64 Seaglidors are actuated only by a VBD and pitch and roll control mechanisms,
65 which work by shifting and rotating the battery pack. The glider has a shape
66 that is hydrodynamically optimised for least drag at its operating speed of
67 approximately 0.25 m/s horizontal velocity, which is achieved through its
68 wings. Seaglidors are rated for depths of 1,000 m and a deeper water version
69 has also been developed, the Deepglider, which can dive up to 6,000 m deep
70 (Osse and Eriksen, 2007).

71 Although UGs may perform steady-state spiralling motions as shown by
72 Zhang et al. (2013), the NOC runs missions with the Seaglidors performing
73 the classical sawtooth profiles in the vertical plane. In order to ensure high
74 quality of the scientific measurements, a symmetrical dive pattern is desired,
75 i.e. the Seaglider should present a similar mean glide slope for both dive and
76 climb and little standard deviation (IRobot, 2012). Additionally, whereas the
77 UG is designed to roll to achieve the desired yaw angle, roll motions severely
78 affect the measured scientific data for up to 12 s after the roll control is set to
79 zero (Frajka-Williams et al., 2011). Therefore, it is particularly important to
80 trim the UG correctly. Procedures for the determination of the centres of the
81 VBD, pitch and roll control mechanisms have been developed by Williams
82 et al. (2008) for Slocum UGs, which are described in Webb et al. (2001) and
83 Schofield et al. (2007), using system identification strategies on the gliders'
84 deployment data. Similar strategies have been created by the developers
85 of Seaglidors at the University of Washington and these practical solutions
86 can be found in the training manuals for pilots, e.g. the one by IRobot
87 (2012). Furthermore, the control system on-board the Seaglider relies on a

88 dynamic model of the UG, similar to the one described in Leonard and Graver
89 (2001). In order to improve the performance of the UG, it is important
90 to determine the correct model parameters, which are typically labelled as
91 regression parameters (as they are obtained through a regression process)
92 (IRobot, 2012) but are referred to here as flight parameters. Graver and
93 Bachmayer (2003), Graver (2005) and Williams et al. (2008) obtained the
94 lift and drag coefficients for a Slocum UG assuming planar motions, while
95 Merckelbach et al. (2010) extended these methods to estimate vertical water
96 velocities. Eriksen et al. (2001) developed a similar iterative procedure to
97 obtain the lift, drag and induced drag coefficient for a Seaglider based on
98 the equations describing its steady-state motion representative of its low-
99 drag design. This process has been extended to the additional determination
100 of the UG’s compressibility, reference volume and thermal expansivity in
101 Frajka-Williams et al. (2011) for the estimation of vertical currents based on
102 the Seaglider’s measurements.

103 Although innovative control strategies for UGs have been developed since
104 the development of Seagliders, e.g. as described by Mahmoudian and Woolsey
105 (2008), Hussain et al. (2011) and Li and Su (2016), the aim of the fleet
106 management software being developed by the NOC is to optimise the UGs’
107 performance without modifying the control software installed on the devices.
108 As a result, the recommender system will be limited to the determination
109 of the trim and flight parameters of Seagliders based on the analysis of live-
110 stream data. Additionally, a robust implementation is desired in the short
111 term. As a result, an evolution of the well-understood methods based on
112 the equations of motion of a Seaglider under planar steady-state motions is
113 preferred over machine-learning methods. In fact, since the determination
114 of the trim and flight parameters is iterative even for pilots, apprenticeship
115 learning strategies, as for instance described in Abbeel et al. (2010) may not
116 be used successfully in this application.

117 The methods for the determination of the trim and flight parameters are
118 developed using data from actual Seaglider deployments, extending previous
119 work in Anderlini et al. (2019). Additional data were requested from the
120 Australian Integrated Marine Observing System (IMOS) to assess the per-
121 formance of the recommender system for a wide range of deployment sites,
122 surface water temperature and Seaglider devices. Firstly, the determination
123 of the centres of the trim and roll centres is improved with the analysis of
124 raw control points. Then, the estimates of the flight parameters for different
125 dive cycles are smoothed out through improved data cleaning and a larger

126 moving window. Finally, a greater number of missions are analysed to assess
127 the performance of the recommender system against professional UGs' pilots.
128 The following sections will describe the data employed to develop and test
129 the recommender system, the generated procedure followed by a comparison
130 of the output of the recommender system against trim and flight parameters
131 selected by the pilots.

132 2. Seagliders Data

133 2.1. Seagliders

134 During a deployment, a Seaglider, shown in Figure 1, stores a number of
135 time signals and log parameters. In this study, only the time signals used
136 directly in the control of the UG are of interest, rather than the scientific
137 measurements which are the UG's primary mission objective. The basic time
138 series signals can be seen in Table 1, while Table 2 shows the signals derived
139 from the elementary ones. A right-hand-side reference system is used, with
140 positive vertical displacement being upwards. The mean sample period for all
141 deployments is approximately 30 s. [Ranges for the basic variables can be seen](#)
142 [in Table 1 as taken from deployments and IRobot \(2012\).](#) Seagliders have a
143 [typical horizontal velocity of 0.25 m/s and vertical velocity of 0.1-0.15 m/s.](#)



Figure 1: Seaglider UG at the NOC. The antenna has been removed for storage.

Table 1: Basic time series signals used in the recommender system with corresponding typical ranges. The control input variables are expressed in analogue-to-digital counts (0-4095) and their limits are taken from IRobot (2012).

Signal	Symbol	Unit	Typical Minimum Value	Typical Maximum Value
Time	t	[s]	0	18,000
Vertical position	z	[m]	0	1,000
Roll angle	ϕ	[°]	-40	40
Pitch angle	θ	[°]	-40	40
Yaw angle	ψ	[°]	-180	180
Water density	ρ	[g/cm ³]	1.000	1.0275
Water pressure	p	[dbar]	1	101.5
Water temperature	T	[°C]	2	30
Roll control	ϕ_c	[°] or [A/D]	150 A/D, -52°	3833 A/D, 52°
Pitch control	θ_c	[cm] or [A/D]	70 A/D, -10.3 cm	3352 A/D, 10.3 cm
VBD volume	V_{vbd}	[cm ³] or [A/D]	205 A/D, 557 cm ³	3510 A/D, -266 cm ³

Table 2: Derived time series signals used in the recommender system.

Signal	Symbol	Unit
Buoyancy	B	[N]
Vertical velocity	\dot{z}	[m/s]
Vertical acceleration	\ddot{z}	[m/s ²]
Roll velocity	$\dot{\phi}$	[°/s]
Pitch velocity	$\dot{\theta}$	[°/s]
Yaw rate	$\dot{\psi}$	[°/s]

144 Example time series data for a typical dive profile can be seen in Figure 2.
145 In Figure 2a, the typical sawtooth dive profile is clear from the Seaglid-
146 ers vertical position. In Figure 2b-c, during the dive, the vertical velocity, VBD
147 volume, buoyancy, the pitch control and pitch angle signals are all negative
148 and during the climb positive. As evident from Figure 2d, the Seaglider has
149 to roll to maintain the desired heading. However, it is important to notice
150 that the Seaglider turns in the opposite direction from its roll angle on the
151 dive and in the same direction as its roll angle on the climb. This is due
152 to the position of the centre of the hydrodynamic forces and the orientation
153 of the hydrostatic, lift and drag forces in dives and climbs, as described
154 in IRobot (2012). In all analysed deployments, a bang-bang control was
155 used, where the battery pack is rolled by 40° until the desired heading is
156 achieved. This causes significant noise in the other measurements, with a
157 settling time of at least 12 s after the battery pack is rotated back to the zero
158 position (Frajka-Williams et al., 2011). Despite the dynamic effects, bang-
159 bang control is currently preferred in operational practices over smoother
160 proportional control, since it results in lower power consumption and thus
161 longer deployment duration.

162 UGs are sometimes trimmed incorrectly, especially during the initial stages
163 of a deployment. In this case, the curve of the variation in depth with time is
164 no longer symmetrical between dive and climb and it can show a non-linear
165 shape, as shown in Figure 3. Additionally, as can be seen from a comparison
166 between Figure 2a and Figure 3a, the glider spends more time at the apogee
167 trying to pitch upwards and climb. This is clearly reflected in Figure 3b and
168 Figure 3c, where both the vertical velocity and pitch angle signals do not
169 respond linearly to changes in the control input. In the worst case scenario,
170 the Seaglider has been observed to climb vertically to the surface tail up.

171 2.2. Steady-State Dynamic Model of a Seaglider

172 Zhang et al. (2013) have shown that UGs may be operated in a spiralling
173 motion in steady-state conditions. Furthermore, as described by Rudnick
174 (2016), UGs can provide measurements at a specific location by profiling
175 vertically in the water against ocean currents with steep glide slopes. How-
176 ever, the data analysed in this article concerns the classical operation of
177 Seaglid-ers as profiling the water with a typical sawtooth pattern with a glide
178 angle ranging from 10° to 45° , with 18° being the angle corresponding to
179 greatest efficiency (Davis et al., 2003).

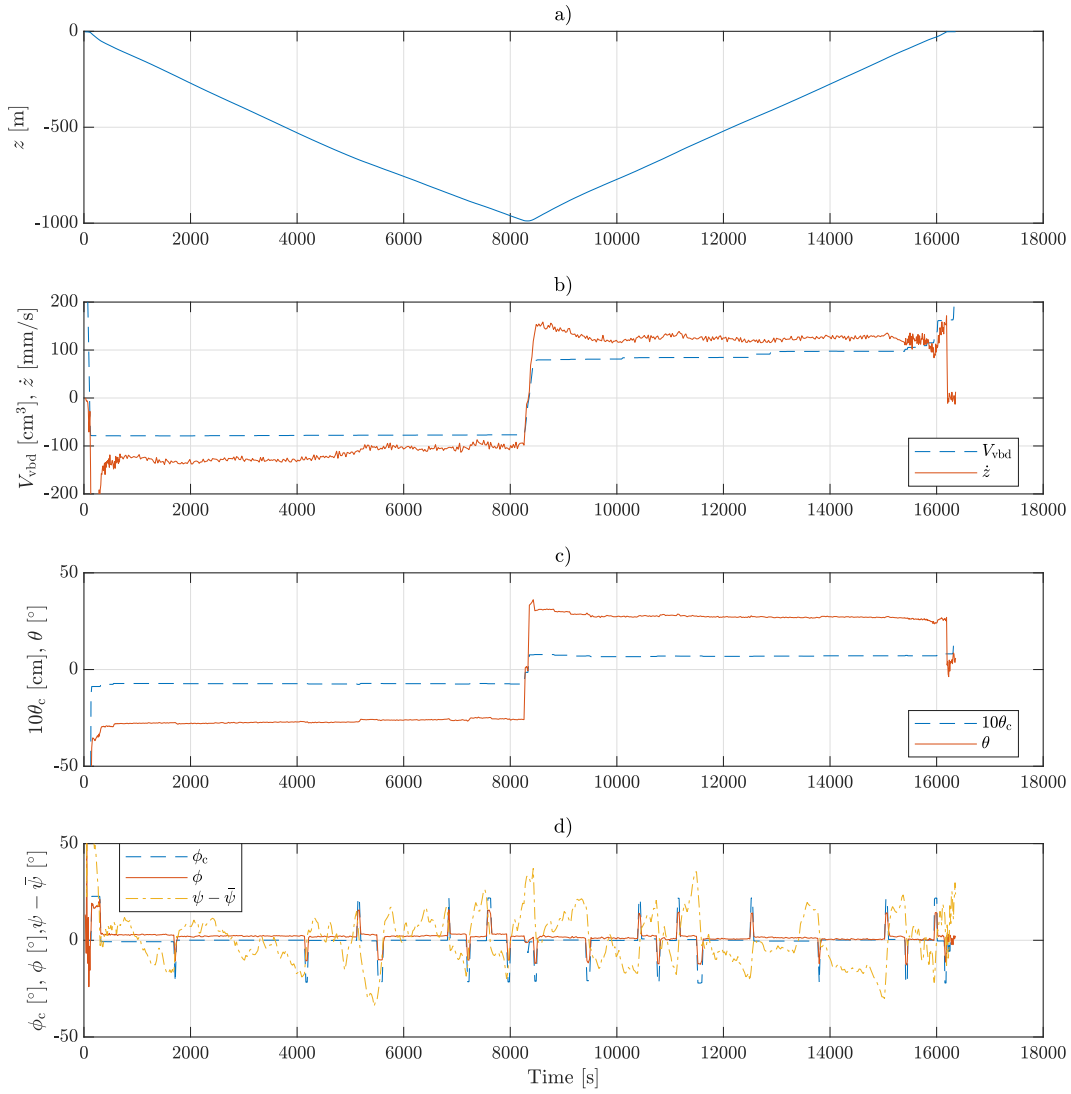


Figure 2: Example dive profile of a correctly trimmed glider.

180 The dynamic model of a Seaglider in planar motions in the vertical plane
 181 under steady-state conditions has been described by Eriksen et al. (2001) and
 182 Frajka-Williams et al. (2011). A free-body diagram is reported in Figure 4
 183 for clarity. Under these assumptions and due to the hydrodynamic shape of
 184 the hull, the UG dynamics can be described by the following equations from
 185 a balance of forces:

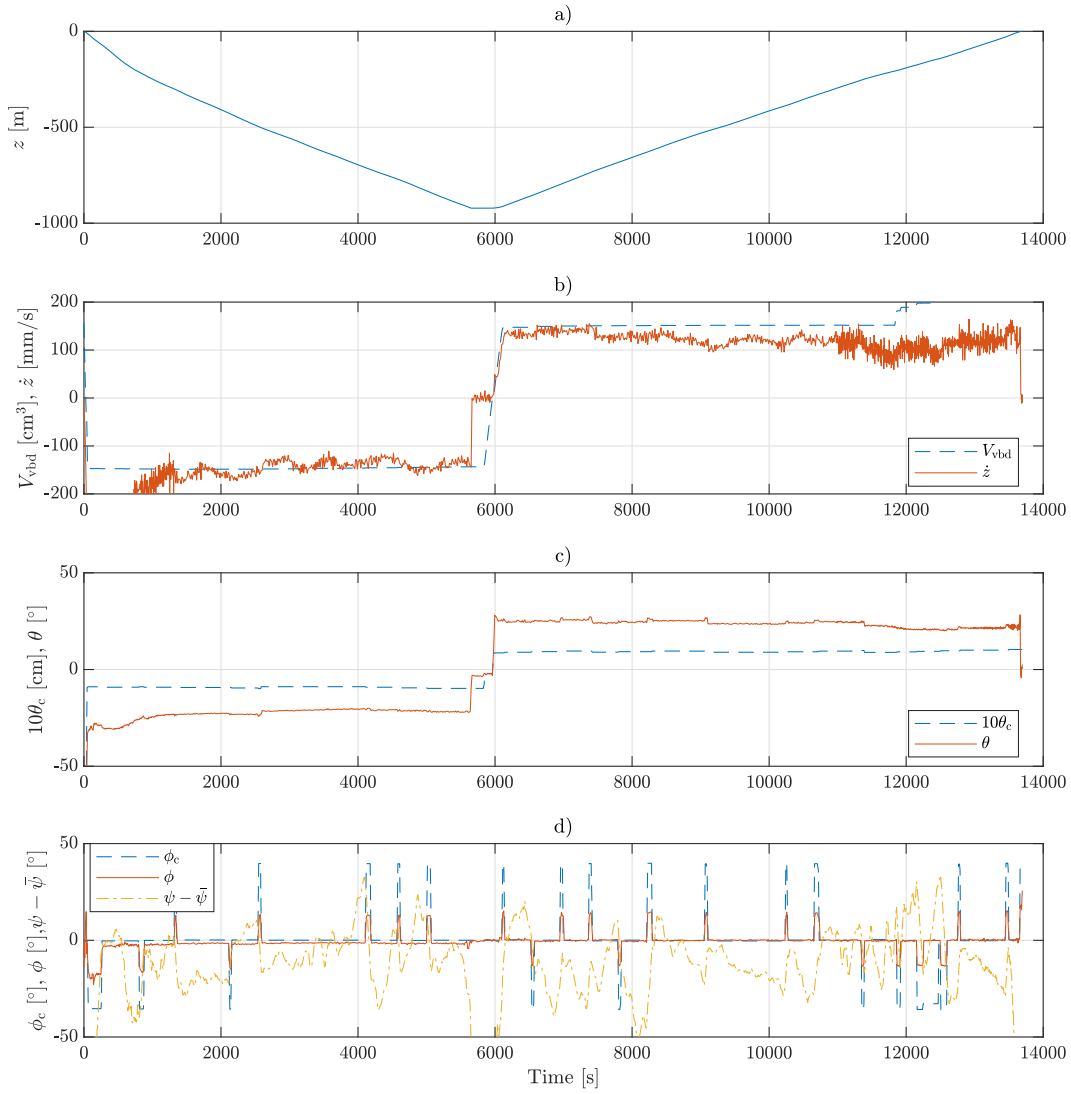


Figure 3: Example dive profile of an incorrectly trimmed glider.

$$L = al^2q\alpha = -B \cos \beta, \quad (1a)$$

$$D = l^2q (bq^{-0.25} + c\alpha^2) = B \sin \beta, \quad (1b)$$

186 where L [N] and D [N] are the lift and drag forces, respectively, l the length
 187 of the UG (1.8 m for Seaglidors, ignoring the antenna) and a [deg^{-1}], b [$\text{N}^{0.25}$]

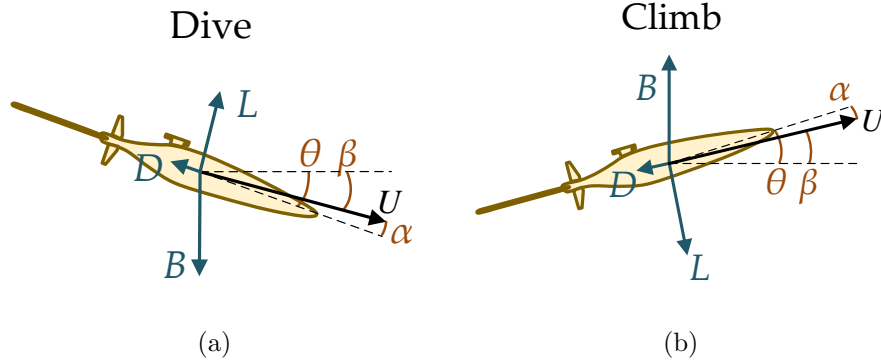


Figure 4: Free-body diagram of the Seaglider in the vertical plane under steady-state conditions in a dive (a) and climb (b). B , D and L indicate the buoyancy, drag and lift forces, respectively, and α , β and θ the attack, glide and pitch angles, respectively.

188 and c [deg^{-2}] are the lift, drag and induced drag hydrodynamic coefficients,
 189 respectively. The units of the drag coefficient are due to the shape of the
 190 Seaglider, which ensures a laminar flow over the length of the UG up to the
 191 point when it tapers down into the antenna. As a result, drag scales with
 192 the speed in the water to the power of 1.5 instead of the typical 2 (Frajka-
 193 Williams et al., 2011). α [$^\circ$] is the angle of attack and $\beta = \theta - \alpha$ [$^\circ$] the glide
 194 slope angle. The dynamic pressure is $q = \rho(u^2 + w^2)/2$, where u [cm/s] and
 195 w [cm/s] are the horizontal and vertical velocity, respectively. The buoyancy
 196 force can be calculated as

$$B(t) = g [-m + \rho(t)\nabla(t, p, T)], \quad (2)$$

197 where m [g] is mass of the UG and $g = 9.81 \text{ m/s}^2$ the gravitational acceler-
 198 ation. The volume displaced by the Seaglider is computed as

$$\nabla(t, p, T) = [V_0 + V_{\text{vbd}}(t)] \exp\{-\gamma_g p(t) + \alpha_g [T(t) - T_0]\}, \quad (3)$$

199 where the reference temperature is set to $T_0 = 0^\circ\text{C}$ for simplicity (this means
 200 that degrees Celsius are used as unit instead of Kelvin - it is important to
 201 note that this does not correspond to the temperature at which the UG
 202 reference volume is taken), V_0 [cm^3] is the reference volume of the Seaglider,
 203 γ_g [dbar^{-1}] the absolute compressibility of the UG and α_g [$1/^\circ\text{C}$] its thermal
 204 expansivity.

205 From (1a) and (1b), it is possible to obtain the following two equations
 206 for the dynamic pressure, q , and angle of attack, α , respectively,

$$q = \frac{B \sin \beta q^{0.25}}{2l^2 b} \left(1 + \sqrt{1 - \frac{4bc}{\alpha^2 \tan^2 \beta q^{0.25}}} \right), \quad (4a)$$

$$\alpha = -\frac{\alpha \tan \beta}{2c} \left(1 + \sqrt{1 - \frac{4bc}{\alpha^2 \tan^2 \beta q^{0.25}}} \right). \quad (4b)$$

207 Both (4a) and (4b) are implicit and thus require an iterative solution.
 208 Additionally, a check is needed to ensure the **argument to the radical** is
 209 positive; otherwise the data point will need to be discarded.

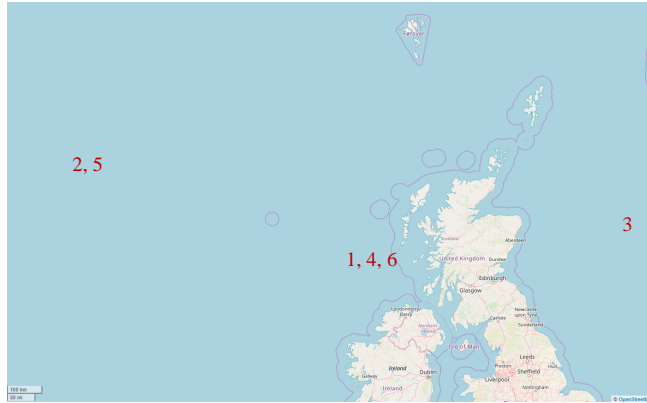
210 The vertical velocity predicted by the dynamic model, \dot{z}_m , is therefore

$$\dot{z}_m \approx w = \frac{2}{\rho} q \sin(\theta - \alpha) = \frac{2}{\rho} q \sin \beta. \quad (5)$$

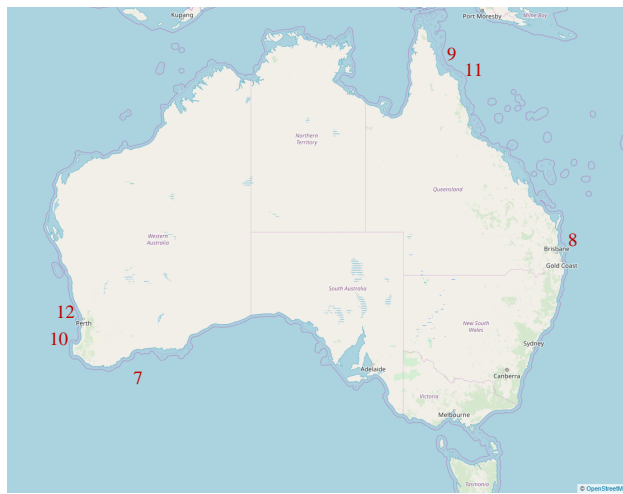
211 Note that the vertical velocity must be then converted to [m/s].

212 2.3. Dataset

213 This study involved the analysis of the data measured by Seaglid^{ers} dur-
 214 ing 12 missions. The Seaglid^{ers}' deployments data have been taken from
 215 two main sources: the NOC **and the Scottish Association for Marine Science**
 216 **(SAMS)** in the UK (6 deployments) and the IMOS in Australia (6 deploy-
 217 ments). Figure 5a and Figure 5b display the geographical position of the
 218 missions run by the NOC and IMOS, respectively. The Seaglider identity
 219 number, location, maximum target depth, mean surface temperature at the
 220 surface and number of dive cycles for the analysed deployments can be seen
 221 in Table 3. Whereas all missions present a maximum target depth close the
 222 rated depth of Seaglid^{ers} (1000 m), the water temperature at the surface
 223 varies significantly with geographical location. This is expected to have con-
 224 sequences on the marine growth levels on Seaglid^{ers} due to the UG's long
 225 missions, which each dive cycle lasting 4 to 8 hours. From Table 3, it is also
 226 possible to notice that the NOC **typically** operates the Seaglid^{ers} for longer
 227 deployments.



(a)



(b)

Figure 5: Location of the Seagliders deployments run by the (a) **NOC/SAMS** and (b) IMOS used in the dataset.

228 **3. Recommender System**

229 In order to achieve symmetrical dive profiles for high quality scientific
 230 measurements and to reduce power consumption, it is important to determine
 231 the trim and flight parameters of the Seaglider. Currently, these parameters
 232 are obtained by pilots using the data collected during the UG’s deployment

Table 3: Seaglider identity number, mission location, maximum target depth ($d_{\text{tgt,max}}$), mean temperature at the surface ($\overline{T_s}$) and number of dive cycles for all deployments in the analysed dataset. The mission duration is extracted from the GPS fix readings.

Dep. ID	Organisation	UG ID	Location	$d_{\text{tgt,max}}$ [m]	$\overline{T_s}$ [°C]	No. dive cycles	Mission duration [days]
1	NOC/SAMS	sg545	Hebrides	990	12.2	886	16.8
2	NOC/SAMS	sg532	North Atlantic	990	9.5	994	176.9
3	NOC/SAMS	sg550	North Sea	1000	10.3	1147	44.1
4	NOC	sg616	Hebrides	990	10.8	1667	165.9
5	NOC/SAMS	sg603	North Atlantic	990	10.2	1350	175.6
6	NOC/SAMS	sg602	Hebrides	990	12.6	1604	143.8
7	IMOS	sg153	Bremer Bay	990	19.8	268	33.7
8	IMOS	sg516	Brisbane	990	25.8	668	91.3
9	IMOS	sg514	Coral Sea	990	25.7	482	103.4
10	IMOS	sg516	Leeuwin	990	22.7	600	66.9
11	IMOS	sg540	Lizard Island	990	32.8	229	36.4
12	IMOS	sg514	Perth	990	21.0	699	107.9

233 based on manuals and procedures developed by the Seagliders developers
 234 (Eriksen et al., 2001; Frajka-Williams et al., 2011; IRobot, 2012). Here a
 235 recommender system is developed, which is designed to have a similar level
 236 of performance to expert pilots. Since the NOC is to implement the system
 237 on their UGs fleet control and command software soon, high robustness and
 238 a similarity to existing procedures are desired of the recommender system.
 239 For this reason, the existing strategies relying on steady-state conditions
 240 assumptions developed by Eriksen et al. (2001), Frajka-Williams et al. (2011)
 241 and IRobot (2012) have been adopted and improved upon.

242 3.1. Algorithm

243 The algorithm used for the recommender system of the trim and flight
 244 parameters of Seagliders is summarised in Figure 6. Furthermore, Figure 6
 245 clearly delineates the different stages of the data preparation, parameters
 246 determination and update.

247 In an actual deployment, there is a time lag of two dive cycles in the
 248 update of the estimated trim and flight parameters due to the actual time
 249 required to process the data from the new run. Let us consider dive cycle
 250 i . After the dive cycle is completed, the data will be processed to obtain
 251 the new flight and trim parameters. However, the new parameters cannot be
 252 set for dive cycle $i + 1$, since the processing will take some time and when
 253 the Seaglider connects to the command and control software by satellite
 254 communication, it already requires new values. As a result, the update to
 255 the coefficients using the data from dive cycle i will be available only for dive
 256 cycle $i + 2$.

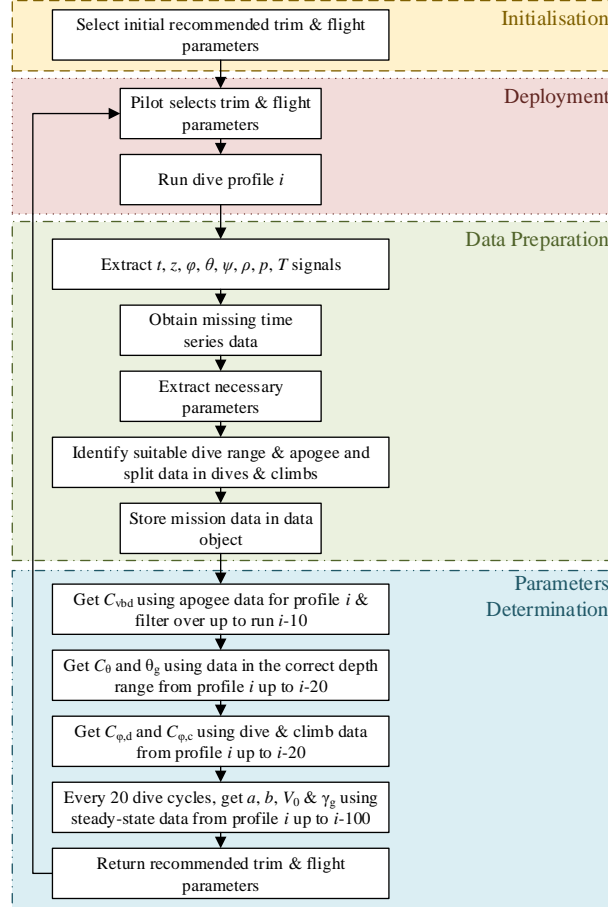


Figure 6: Workflow of the recommender system for the estimation of the trimming and flight parameters of Seaglidert.

257 3.2. Trim Parameters

258 A UG needs to be trimmed correctly so that it can take scientific mea-
 259 surements at regular intervals in space and time on the desired path. The
 260 trimming operation consists in the correct zeroing of the pitch and roll con-
 261 trol mechanisms and of the VBD by finding their respective actual centres,
 262 namely C_θ , $C_{\phi,d}$, $C_{\phi,c}$ and C_{vbd} , respectively (note that the roll control mech-
 263 anism has a different centre for dives and climbs due to the top-bottom
 264 asymmetry of Seaglidert because of appendages for scientific measurements).
 265 **Based on pilots' observations, the values of the centres typically vary by ap-**

266 proximately 15% for a Seaglider within a single mission and by up to 20% for
267 different vehicles even for similar payload. Hence, their correct determination
268 and the tracking of any changes are particularly important. Furthermore, the
269 gain for the pitch control mechanism, θ_g , must also be estimated, which de-
270 scribes the change in pitch angle that corresponds to a linear displacement of
271 1 cm of the battery pack. The values of the centres are then converted into
272 analogue/digital (A/D) units for the controller on board the Seaglider using
273 appropriate conversion factors. This section describes how the centres of the
274 VBD, pitch and roll control mechanisms are determined in the recommender
275 system.

276 At the moment, a pilot determines the trim parameters during the first
277 10-20 dive profiles and subsequently updates them whenever necessary using
278 software provided by the UG's manufacturer. Current practice dictates that
279 the centres of the VBD and pitch control mechanisms should be determined
280 first, since they have the strongest impact on the UG's trim and performance
281 (IRobot, 2012). Subsequently, the roll control mechanism may be zeroed.

282 A similar approach is followed in the recommender system. Initially, the
283 default values for C_θ , $C_{\phi,d}$, $C_{\phi,c}$ and C_{vbd} , which may be found in IRobot
284 (2012), are returned. Then, the following methods are applied to estimate
285 the actual trim parameters. The procedures are repeated throughout the
286 glider deployments so that the parameters are constantly updated.

287 3.2.1. Determination of the VBD centre

288 After the Seaglider performs a dive profile, the position of the centre of
289 the VBD is updated by analysing the difference in the zero-crossing time of
290 the vertical velocity and VBD control signals as shown in Figure 2b. If the
291 system were perfectly balanced, both signals would cross zero at the same
292 time at the apogee, or lowest point, of the profile. If this is not the case,
293 C_{vbd} is corrected by the magnitude of V_{vbd} at the time step when $\dot{z} = 0$. In
294 the case of a well-calibrated system, e.g. as displayed in Figure 2, finding
295 the point for which $\dot{z} = 0$ is relatively simple, despite the Seaglider collecting
296 data points more frequently in the apogee region. Conversely, for incorrectly
297 trimmed UGs, i.e. during the initial deployment stages, the glider may spend
298 a long time changing from a downward to an upward glide, as can be seen
299 in Figure 3. As a result, the point corresponding to the greatest depth is
300 selected as the point for which $\dot{z} = 0$ occurs. With increasing number of dive
301 cycles and hence updates to the estimate of C_{vbd} , this approach has been
302 found to quickly lead to convergence to the expected VBD centre.

303 After analysing the deployments data, only 50% of the expected correc-
 304 tion to C_{vbd} is applied as recommended by IRobot (2012) to pilots. The
 305 reason for this is the effect of the coupling of the VBD and pitch control cen-
 306 tres on the UG’s trim. Further filtering and activation functions are applied
 307 to reduce noise in the estimation of the centre of the VBD. **Simple digital**
 308 **filters are used in this study, with different window sizes for the the various**
 309 **control mechanisms, as described in the appendix. The adjustments for the**
 310 **determination of the VBD centre** are explained in detail in Appendix A.

311 3.2.2. Determination of the pitch centre and gain

312 To determine C_θ and θ_g the data corresponding to shallow depths and near
 313 the apogee are discarded. This means that only the data points corresponding
 314 to a vertical position in the following range are kept:

$$\min z + \min(|0.1 \min z|, 50 \text{ m}) < z < -\min(|0.1 \min z|, 50 \text{ m}). \quad (6)$$

315 After one dive profile, the variation of the pitch angle with pitch control
 316 input is plotted as in Figure 7. Whereas in IRobot (2012) and Anderlini et al.
 317 (2019) the pitch control displacement in cm is considered, here the raw A/D
 318 values is used instead. This enables us to amalgamate data from a number
 319 of past dive cycles, thus speeding up convergence to the correct pitch centre
 320 and gain, even if the input C_θ and θ_g values are different. However, due to
 321 the effect of the coupling of the VBD and pitch control mechanism on the
 322 pitch angle of the Seaglider, only past data with the *same* C_{vbd} input may be
 323 accumulated as can be seen in Figure 7. The data are then fitted with a line,
 324 whose offset and slope can be used to determine the estimate of the pitch
 325 centre and gain. The slope yields θ_g after multiplication by the conversion
 326 factor from A/D to cm. The abscissa of the point where the line crosses
 327 $\theta = 0^\circ$ corresponds to C_θ .

328 Like for C_{vbd} , accumulation, filtering and activation functions are used
 329 to reduce noise in the estimation of C_θ and θ_g . These are summarised in
 330 Appendix B.

331 3.2.3. Determination of the roll centres

332 The procedure to estimate the centres of the roll mechanism is similar
 333 to the one used to determine C_θ , with the variation of roll angle with roll
 334 control visible in Figure 8. However, the data is split into dive and climb,
 335 since Seagliders are top and bottom asymmetric. Additionally, similarly to
 336 the determination of the pitch centre, only the data points corresponding

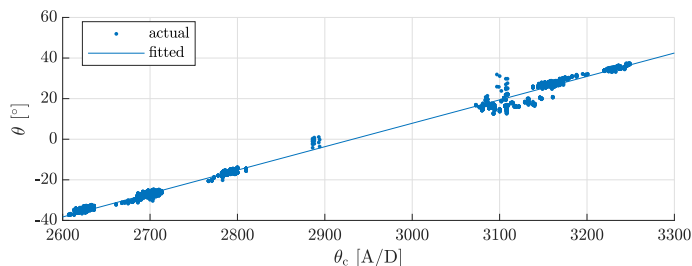


Figure 7: Variation of pitch angle with pitch control for an example dive profile.

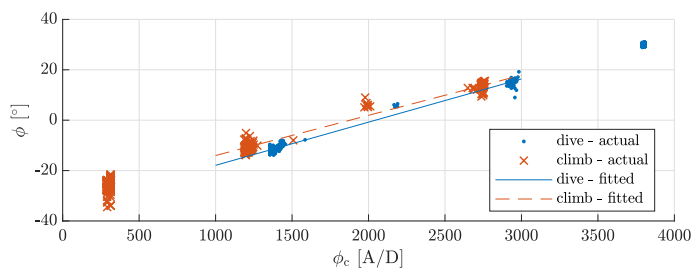


Figure 8: Variation of roll angle with roll control for the dive and climb (b) for an example dive profile.

337 to a vertical position described by (6) are kept. Furthermore, values corre-
 338 sponding to $\phi < 5^\circ$ are ignored. This removes the cluster of points for $\phi \approx 0^\circ$
 339 corresponding to planar motions, but severely affected by disturbances due
 340 to ocean currents. Thus, ignoring the data points for $\phi < 5^\circ$ greatly improves
 341 the quality of the linear fit to the roll data by focusing only on the rolling
 342 motions.

343 Similarly to C_θ , accumulation, filtering and activation functions are used
 344 to reduce noise in the estimation of $C_{\phi,d}$ and $C_{\phi,c}$. These are summarised in
 345 Appendix C.

346 3.3. Flight Parameters

347 In addition to the trim parameters, the pilots can also change some input
 348 parameters to the on-board flight model to optimise the Seaglider perfor-
 349 mance, which is based on the steady-state equations of motion (1-5). The
 350 main flight parameters with the respective initial values (Frajka-Williams
 351 et al., 2011) are

- 352 • hydrodynamic lift coefficient, $a = 0.003836 \text{ deg}^{-1}$,

- 353 • hydrodynamic drag coefficient, $b = 0.010078 \text{ N}^{0.25}$,
- 354 • hydrodynamic induced drag coefficient, $c = 2.1 \times 10^6 \text{ deg}^2$,
- 355 • glider absolute compressibility, $\gamma_g = 4.4 \times 10^6 \text{ dbar}^{-1}$,
- 356 • reference volume, $V_0 = m/\rho_0 \text{ [cm}^3\text{]}$, where ρ_0 is the reference water
357 density $\text{[g/cm}^3\text{]}$,
- 358 • glider thermal expansivity, $\alpha_g = 7.05 \times 10^5 \text{ }^\circ\text{C}^{-1}$.

359 The reference density is set as the highest density experienced by the Seaglider
360 and is also used to calculate the expected maximum buoyancy, $B_{\text{max}} \text{ [g]}$.

361 Eriksen et al. (2001) performed a regression analysis to determine a , b
362 and c by minimising the difference of the UG vertical velocity with the one
363 predicted by (5) from 100 dive profiles for a wide range of glide slopes. Simi-
364 larly, Frajka-Williams et al. (2011) determined the hydrodynamic coefficients
365 by combining the data from a whole deployment, although the principal
366 aim of their study was the determination of vertical currents. Additionally,
367 Frajka-Williams et al. (2011) assessed the sensitivity of the vertical velocity
368 of a Seaglider with the flight parameters. Whereas the hydrodynamic lift
369 and drag coefficients cause a change in the vertical velocity of different sign
370 for climbs and dives, a positive change in the reference volume results in a
371 negative change in the vertical velocity for both climbs and dives. Further-
372 more, although the impact of a , b and V_0 on \dot{z} does not vary significantly
373 with depth, the effect of the compressibility varies with depth because of the
374 pressure (note that Seagliders are designed to have almost the same com-
375 pressibility as water). The impact of c and α_g was found to be negligible.
376 However, significant changes in the default value of the induced lift coeffi-
377 cient are possible if the Seaglider presents considerable appendages (Queste,
378 2018). In addition, the default values of a and b , which were obtained in wind
379 tunnel experiments, are also known to vary due to the appendages (Eriksen
380 et al., 2001). As a result, it is current standard practice at the NOC for
381 pilots to run an optimisation to determine a , b , V_0 and γ_g after the first 50
382 dive cycles and subsequently updating them as more dive profiles are run
383 by including the whole dataset. In particular, the optimisation for the pairs
384 a and b and V_0 and γ_g are alternated, as done similarly by Queste (2018).
385 Furthermore, \dot{z}_m and \dot{z} are gridded in the $\theta - B$ search space to reduce the
386 impact of salinity gradients (Frajka-Williams et al., 2011).

387 In order to ensure the robustness of the recommender system and ensure
388 a speedy commissioning, the regression analysis on the steady-state model
389 of the Seaglider is adopted. However, the development of a recommender
390 system for the flight parameters presents a different objective from the study
391 by Frajka-Williams et al. (2011), who tried to estimate vertical ocean cur-
392 rents, whose magnitude is of the order of 1-5 cm/s. Hence, the following
393 modifications have been made:

- 394 • The flight parameters are first determined for the 100th dive cycle and
395 then recalculated every 20 dive cycles using data points accumulated
396 over a number of past dive cycles. Analysing the data from all past
397 dive cycles up to the current one as done by Eriksen et al. (2001) and
398 Frajka-Williams et al. (2011) is undesirable, since changes in system
399 dynamics would not be tracked. This is particularly important for
400 condition monitoring of the UG, since the parameters can be used to
401 identify changes in the system dynamics, e.g. due to marine growth or
402 subsystem failures. Hence, the analysis of data coming from a moving
403 window is preferred. Although Queste (2018) suggests 20 dive cycles
404 could be an appropriate size for the moving window, this value has
405 been found to be too small in this study. Here, the flight parameters
406 are estimated using the data coming from up to 100 past dive cycles to
407 ensure a sufficient number of data points are analysed to smooth out
408 noise and dynamic effects. Finally, although here the flight parameters
409 are updated only every 20 dive cycles due to computational constraints,
410 considering the typical duration of 6-8 hours per dive cycle, it would be
411 possible to compute an updated estimate after every dive cycle instead.
- 412 • Only a , b , V_0 and γ_g are estimated, although c is added to the optimi-
413 sation for Seagliders with large sensory appendages.
- 414 • Instead of running two optimisations for the pairs a and b and V_0 and γ_g ,
415 a single optimisation is run for all parameters. This has been found to
416 speed up and improve the quality of the optimisation due to sensitivity
417 of the vertical speed to the different parameters.
- 418 • As opposed to Frajka-Williams et al. (2011) and Queste (2018), the
419 values of the actual and predicted vertical velocity, i.e. \dot{z} and \dot{z}_m ,
420 respectively, are not gridded in the $\theta - B$ or $\theta - \dot{z}$ space. From the
421 analysis of the data from the NOC and IMOS runs, gridding was found

422 to increase the importance of data points on the edges of the data
 423 clusters around the $\theta \approx \pm 18^\circ$ - $\dot{z} \approx 0.15$ m/s regions, which are outliers
 424 and likely to be caused by dynamic effects that were not removed in
 425 the data cleaning process. The large number of data cycles analysed
 426 within the moving window ensures a sufficient number of points for
 427 both dives and climbs and reduces the impact of salinity gradients.
 428 Assuming the data is normally distributed, higher importance is given
 429 to the predictions in the operational range of the Seaglider during the
 430 mission.

- 431 • The cost function has been simplified to

$$J = \overline{|\dot{z} - \dot{z}_m|}, \quad (7)$$

432 where the bar indicates the mean excluding non-numerical values (nan-
 433 mean in MATLAB). Excluding the non-numerical values is fundamen-
 434 tal, since most grid points are non-numeric. Note also that the cost
 435 function includes points from both dives and climbs, thus resembling
 436 the one developed by Frajka-Williams et al. (2011).

- 437 • In order to ensure the steady-state, planar-motion assumption is met
 438 but at the same time maximise the number of data points available for
 439 the regression analysis, the time series data from the moving window
 440 of 100 dive cycles are cleaned. Firstly, all aborted runs or dive cycles
 441 where the Seaglider climbs tail-up are removed. Additionally, after
 442 taking some inspiration from Queste (2018), only the data points that
 443 meet the following requirements have been kept:

- 444 – depth given by (6) to remove data points close to the surface or
 445 apogee, when nonlinearities are significant,
- 446 – $|\dot{z}| > 0.02$ m/s to remove points when the UG has stalled,
- 447 – $|\ddot{z}| < 0.01$ m/s² to avoid transient conditions,
- 448 – $|\phi| < 2.5^\circ$ to avoid roll angles and their associated coupled and
 449 nonlinear dynamic response,
- 450 – $|\theta| < 45^\circ$ to avoid excessive pitch angles,
- 451 – $|\dot{\phi}| < 1^\circ/\text{s}$ to avoid transient conditions,
- 452 – $|\dot{\theta}| < 1^\circ/\text{s}$ to avoid transient conditions.,

453 – p , T and ρ present numeric values.

454 Additionally, two points have been removed from each side of each
455 segment of good data to further reduce the risk of inclusion of transient
456 data.

457 • Finally, the flight parameters estimated every 20 dive cycles are further
458 filtered over 5 values, which corresponds to 100 dive cycles. Further-
459 more, an activation function is applied, which ensures no change is
460 applied unless

- 461 – $\delta a > 0.001 \text{ deg}^{-1}$,
- 462 – $\delta b > 0.001 \text{ N}^{0.25}$,
- 463 – $\delta c > 2 \times 10^{-6} \text{ deg}^{-2}$,
- 464 – $\delta < \gamma_c > 2 \times 10^{-6} \text{ dbar}^{-1}$,
- 465 – $\delta V_0 > 10^3 \text{ cm}^3$.

466 Whereas the default values are used for α_g and sometimes c , the recom-
467 mender thus finds a , b , V_0 and γ_g (and c for Seaglidors with large appendages)
468 before each new dive profile by minimising (7) using the cleaned data from
469 the past 100 dive cycles. The estimated vertical velocity values are obtained
470 from (2-5), using iterative solutions for (4) up to 15 iteration or as soon as the
471 change in estimated dynamic pressure is less than 0.001. The interior-point
472 algorithm is used for the constrained optimisation using the MATLAB func-
473 tion *fmincon* with the following boundaries (Frajka-Williams et al., 2011):

- 474 • $0.001 \text{ deg}^{-1} < a < 0.007 \text{ deg}^{-1}$,
- 475 • $0.004 \text{ N}^{0.25} < b < 0.02 \text{ N}^{0.25}$,
- 476 • $10^{-6} \text{ deg}^{-2} < c < 3 \times 10^{-5} \text{ deg}^{-2}$,
- 477 • $10^{-6} \text{ dbar}^{-1} < \gamma_c < 3 \times 10^{-5} \text{ dbar}^{-1}$,
- 478 • $5 \times 10^4 < V_0 < 5.5 \times 10^4 \text{ cm}^3$.

479 4. Results and Discussion

480 Figures 9-14 show the comparison of key trim and flight parameters esti-
481 mated by the recommender system as compared with those actually selected
482 by experienced pilots for the deployments run by the NOC and IMOS, which
483 are representative of Seaglider missions in a broad range of oceanographic
484 conditions.

485 From Figures 9-10, it is clear how closely the recommendations match
486 the centres of the VBD and pitch control mechanism selected by the pilots.
487 The same applies to the pitch gain, although it is not shown. The close
488 comparison is expected, since only small improvements have been made over
489 the system employed by the pilots to pick the three trim parameters. The
490 activation and filter functions are successful in smoothing out excessive noise
491 and preventing outliers (e.g. as shown by deployment 2, i.e. Seaglider 532
492 in the North Atlantic). However, the curve for the estimated pitch centre
493 still presents some oscillations, particularly for deployment 10 (Seaglider 516
494 near Leeuwin). These oscillations are mainly due to convergence to local
495 optima. The activation function should be improved to remove this unde-
496 sirable outcome. The oscillations in the recommended value for the pitch
497 value for Seagliders 602 and 603 in Figure 9 are interesting because they are
498 not one-off errors. Hence, they are likely to be physical phenomena due to
499 changes in the weight distribution or malfunctions of the glider towards the
500 end of its deployment. These are reflected by changes in the roll centres in
501 Figure 11 for the same dive profiles.

502 Conversely, the comparison between the roll centres selected by the recom-
503 mender system and the pilots presents stronger differences as in Figures 11-
504 12. The main reason for this behaviour is the removal of all points corre-
505 sponding to $\phi < 5^\circ$ in the recommender system, since they severely affect
506 the quality of the linear fit. Hence, the recommender system is expected to
507 be more precise. Additionally, outliers due to errors in the calculation of the
508 slope and offset of the linear fit are no longer present.

509 For both the data selected by pilots and the recommender system, the
510 values of the roll centres vary more significantly during a deployment as com-
511 pared with the VBD and pitch control centres. This is likely caused by the
512 lower amount of data the fit is based on and the impact of ocean currents,
513 which have much higher horizontal than vertical magnitude (Rudnick, 2016).
514 However, the sudden change in C_θ , $C_{\phi,d}$ and $C_{\phi,c}$ towards the end of a de-
515 ployment may be caused by marine growth affecting the symmetry of the

NOC/SAMS

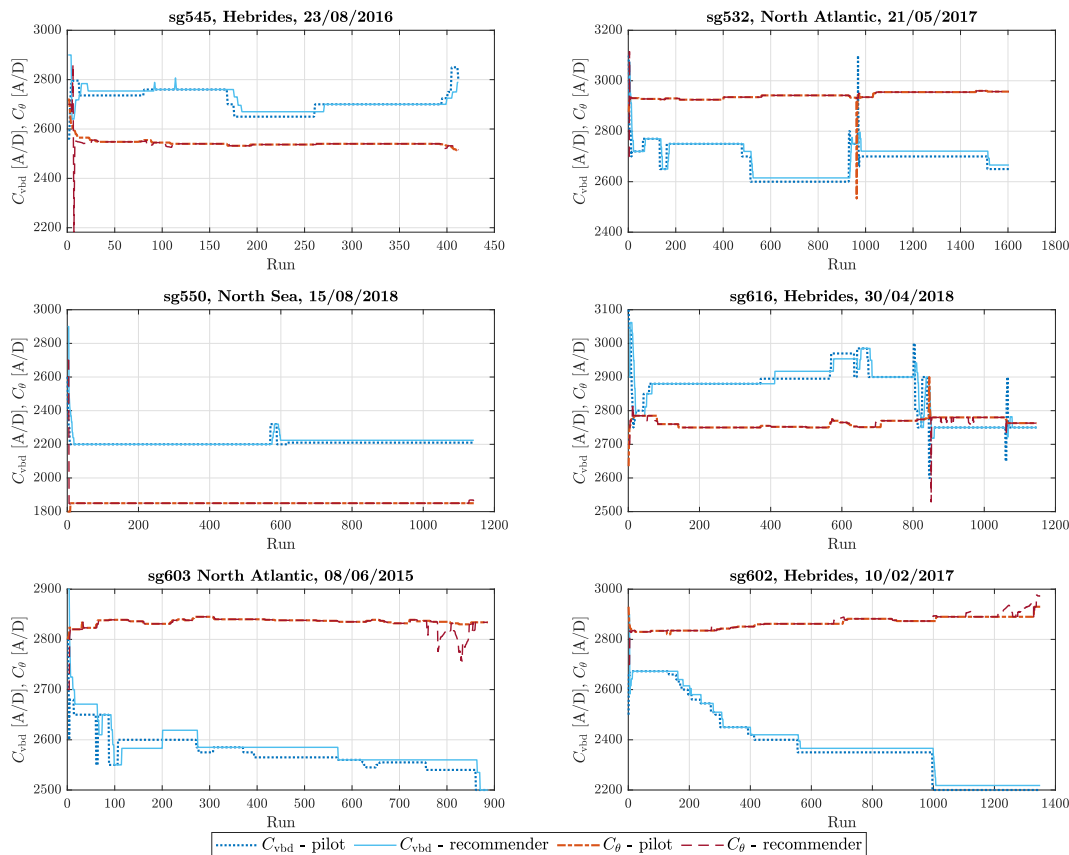


Figure 9: Variation of the centres of the VBD and pitch control mechanism with dive profile as selected by the pilots and recommended by the developed system for the missions run by the **NOC/SAMS**.

516 Seaglider, considering the long duration of the deployments.

517 From Figures 13-14, it is clear that the pilots did not attempt to change
 518 the hydrodynamic coefficients from the nominal values in any of the analysed
 519 deployments. For most missions, the recommender system presents values
 520 close to the nominal values. However, some oscillations can be observed,
 521 which are likely caused by the data sampling within the moving window.
 522 Hence, based on these results the operators will need to assess whether chang-
 523 ing the flight parameters during a mission is desired or whether it is more
 524 appropriate to use fixed parameters, possibly determined from a previous
 525 deployment.

IMOS

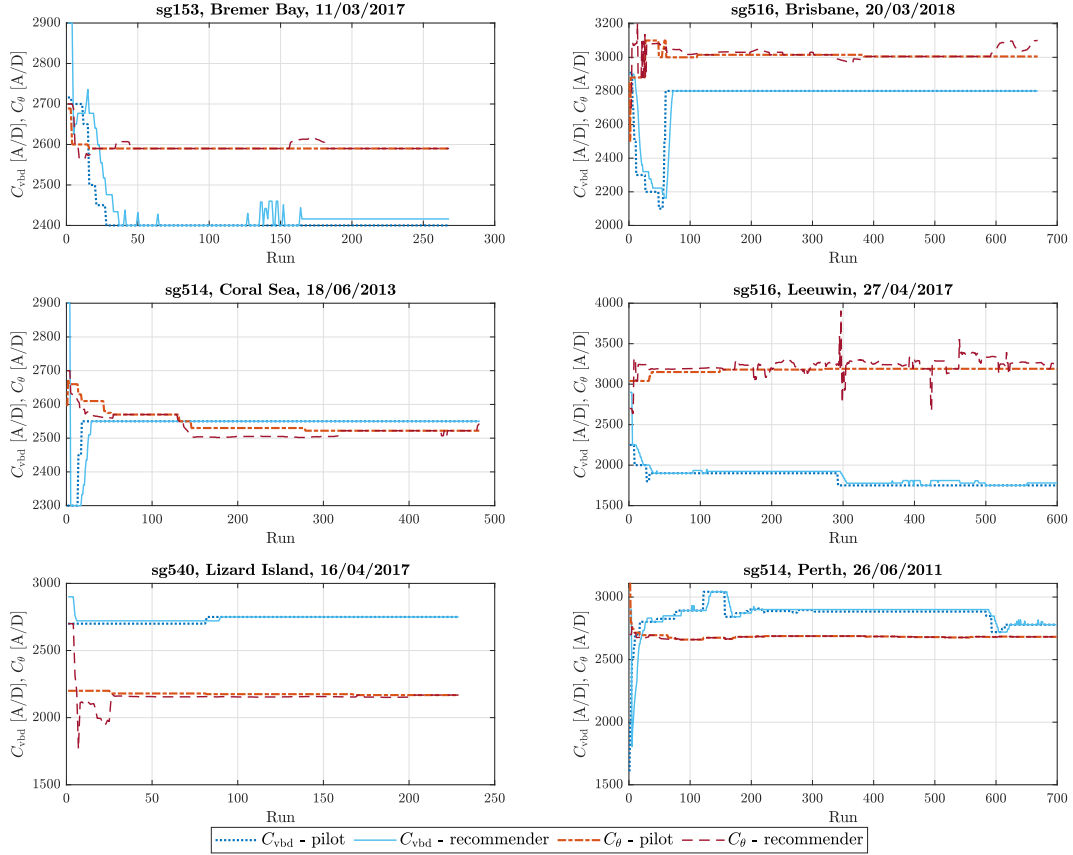


Figure 10: Variation of the centres of the VBD and pitch control mechanism with dive profile as selected by experienced pilots and recommended by the developed system for the missions run by the IMOS.

526 Nevertheless, as can be seen in Figures 13-14, deployments 4 and 8 (i.e.
 527 Seaglidert 616 and 516 deployed near the Hebrides and Brisbane, respec-
 528 tively) show a steep increase in predicted drag coefficient towards the end of
 529 the mission. This is reflected in deployments 5 and 7 (i.e. Seaglidert 603 and
 530 153 in the North Atlantic and Bremer Bay, respectively) to a smaller degree.
 531 This phenomenon is likely to be physical and reflective of marine growth on
 532 the Seaglidert hulls increasing the resistance of their hulls. Hence, the hydrody-
 533 namic coefficients may also be used for the condition monitoring of the device
 534 (although the activation function is not necessary for that application).

535 The difference in the predicted and actually selected trim and flight pa-

NOC/SAMS

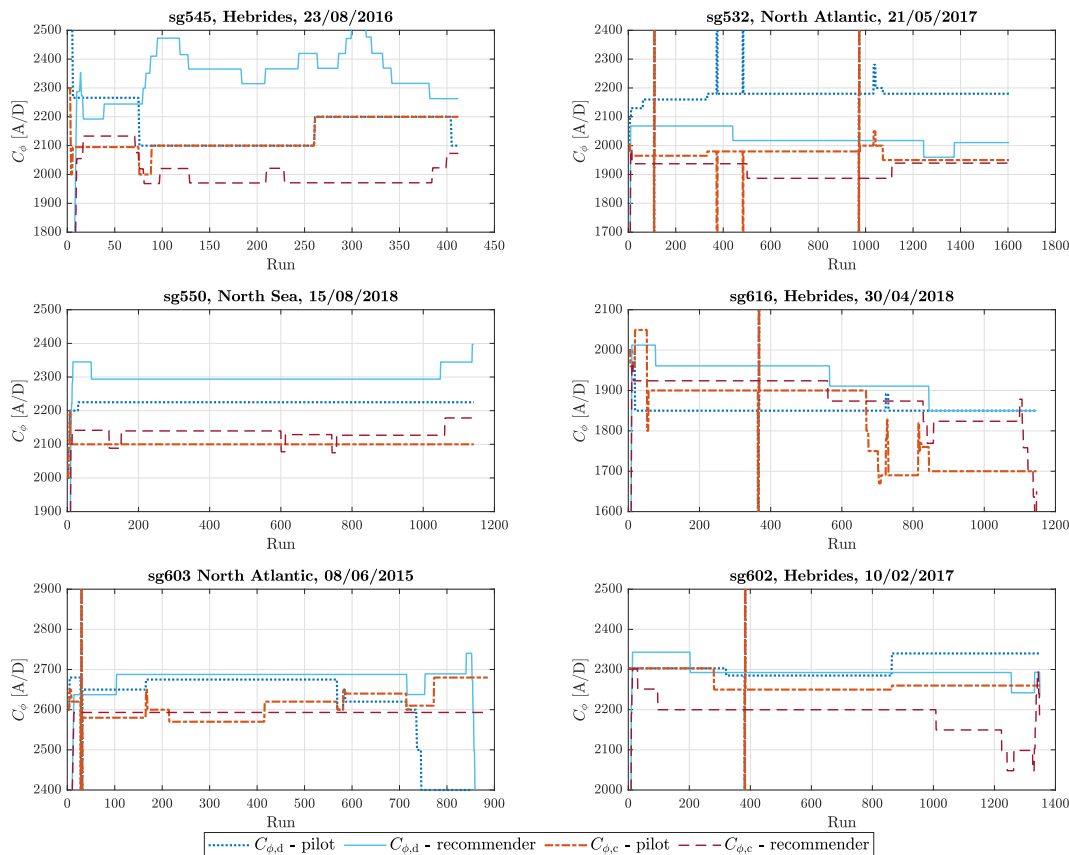


Figure 11: Variation of the centres of the roll control mechanism for dives and climbs with dive profile as selected by experienced pilots and recommended by the developed system for the missions run by the NOC/SAMS.

536 rameters is quantified in Tables 4-5, which display the ratio of the mean
 537 absolute difference and the respective nominal values and the ratio of the
 538 standard deviation of the absolute difference and the corresponding nominal
 539 values, respectively. The tables reflect the trends shown by Figures 9-14.
 540 From Table 4, it is clear that there is excellent agreement between the values
 541 selected by the pilots and the recommender system. However, the estimation
 542 of the roll centres and hydrodynamic coefficients present a mean absolute
 543 percentage difference, which is one to two orders of magnitude greater than
 544 the centres of the VBD and pitch control mechanisms due to the signifi-
 545 cant changes in the procedure used for the data cleaning, linear fit and cost

IMOS

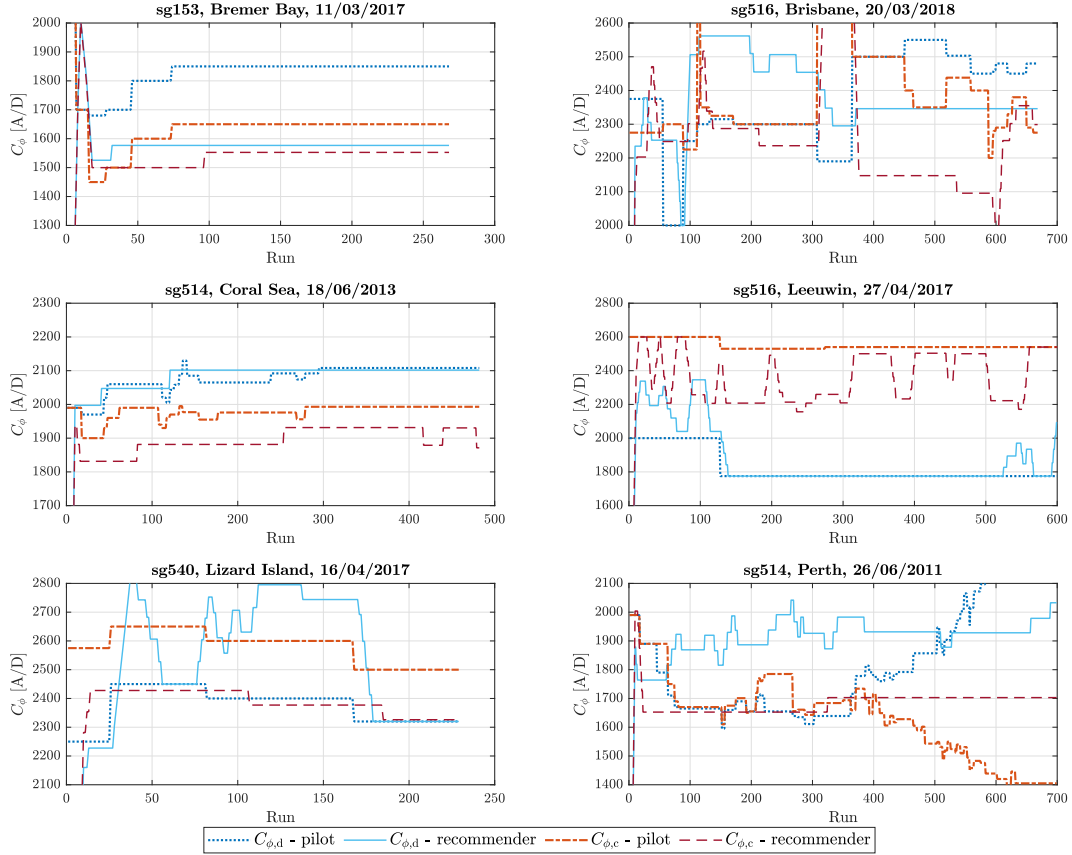


Figure 12: Variation of the centres of the roll control mechanism for dives and climbs with dive profile as selected by experienced pilots and recommended by the developed system for the missions run by the IMOS.

546 function. From Table 5, the standard deviation is more representative of
 547 the visual differences shown in Figures 9-14, since it accounts for changes in
 548 the selected trim and flight parameters with dive cycles. However, Table 5
 549 reflects the trend of Table 4 for the individual parameters.

550 4.1. Suggestions for Operational Practice

551 After the development of the recommender system, the authors would
 552 like to summarise a number of practices that can help with the operation of
 553 Seagliders, particularly for large oceanographic centres.

554 Firstly, the creation of a database for the trim and flight parameters for

Table 4: Mean absolute difference between the prediction of the recommender system and the respective values selected by the pilots divided by the nominal value for the trim and flight parameters.

ID	VBD [%]	θ [%]	ϕ_d [%]	ϕ_c [%]	a [%]	b [%]
1	0.597	0.150	11.163	7.828	5.677	0.000
2	0.619	0.053	8.114	3.178	38.261	8.349
3	0.409	0.131	4.124	2.216	46.335	8.059
4	0.518	0.067	4.066	4.056	33.761	40.384
5	0.569	0.121	4.241	2.725	29.364	16.153
6	0.572	0.180	2.008	4.357	25.384	4.942
7	0.748	0.161	13.689	6.344	26.598	3.833
8	0.605	0.830	9.113	7.697	35.748	34.429
9	0.313	0.496	1.739	4.885	19.099	0.000
10	1.169	2.922	3.310	10.248	6.117	2.336
11	0.405	1.425	10.749	12.167	0.000	3.074
12	1.085	0.124	10.829	6.524	19.197	0.810
mean	0.634	0.555	6.929	6.019	23.795	10.197

Table 5: Standard deviation of the absolute difference between the prediction of the recommender system and the respective values selected by the pilots divided by the nominal value for the trim and flight parameters.

ID	VBD [%]	θ [%]	ϕ_d [%]	ϕ_c [%]	a [%]	b [%]
1	1.187	0.933	12.503	9.096	10.991	0.000
2	0.907	0.680	7.302	7.527	22.131	4.738
3	1.212	1.973	4.890	5.006	22.938	4.890
4	1.177	0.387	6.781	6.900	25.135	41.770
5	0.653	0.443	10.751	9.888	22.500	13.398
6	0.692	0.545	6.457	6.439	21.766	4.545
7	1.324	0.424	10.070	10.987	26.610	7.298
8	2.577	1.481	7.799	9.446	24.649	40.624
9	2.058	0.543	7.380	7.123	15.654	0.000
10	2.118	2.724	8.042	11.049	11.499	4.805
11	0.948	2.941	13.681	13.818	0.000	5.311
12	3.243	0.862	7.181	7.578	19.124	3.337
mean	1.508	1.161	8.570	8.738	18.583	10.893

NOC/SAMS

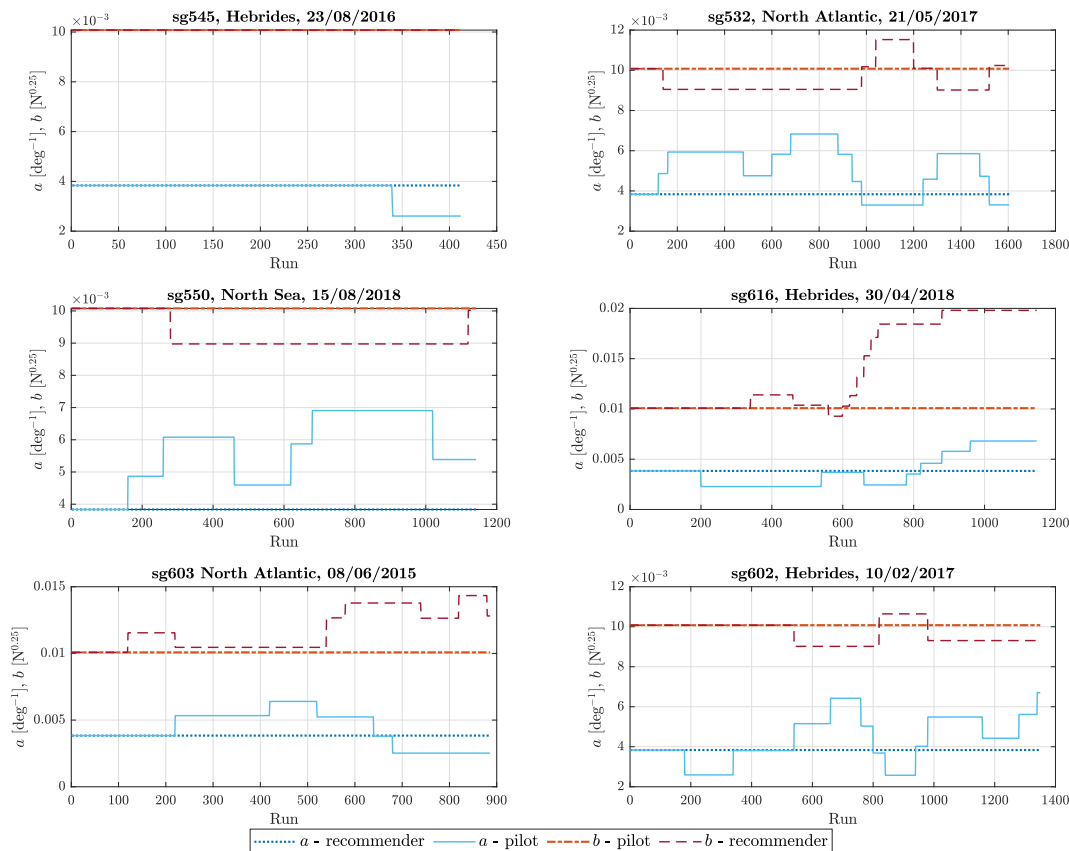


Figure 13: Variation of the lift and drag coefficients with dive profile as selected by the pilots and recommended by the developed system for the missions run by the NOC/SAMS.

555 individual Seagliders and configurations (i.e. the sensors or payloads they
 556 carry) is highly recommended. This would greatly improve the speed and
 557 ease of the initial trimming of the UG. Additionally, the database would
 558 provide a more reliable start point for the recommender system, which would
 559 still be used to track changes in the trim and flight parameters. For instance,
 560 the pressure hull compressibility may change with time. Data on the UGs'
 561 configurations may be used to aid the determination of the trim and flight
 562 parameters for newly commissioned gliders.

563 Secondly, the reference volume may be determined at the surface either
 564 on the mother ship or the facility just before a deployment. This procedure
 565 is standard practice at most oceanographic institutions, like the NOC. This

IMOS

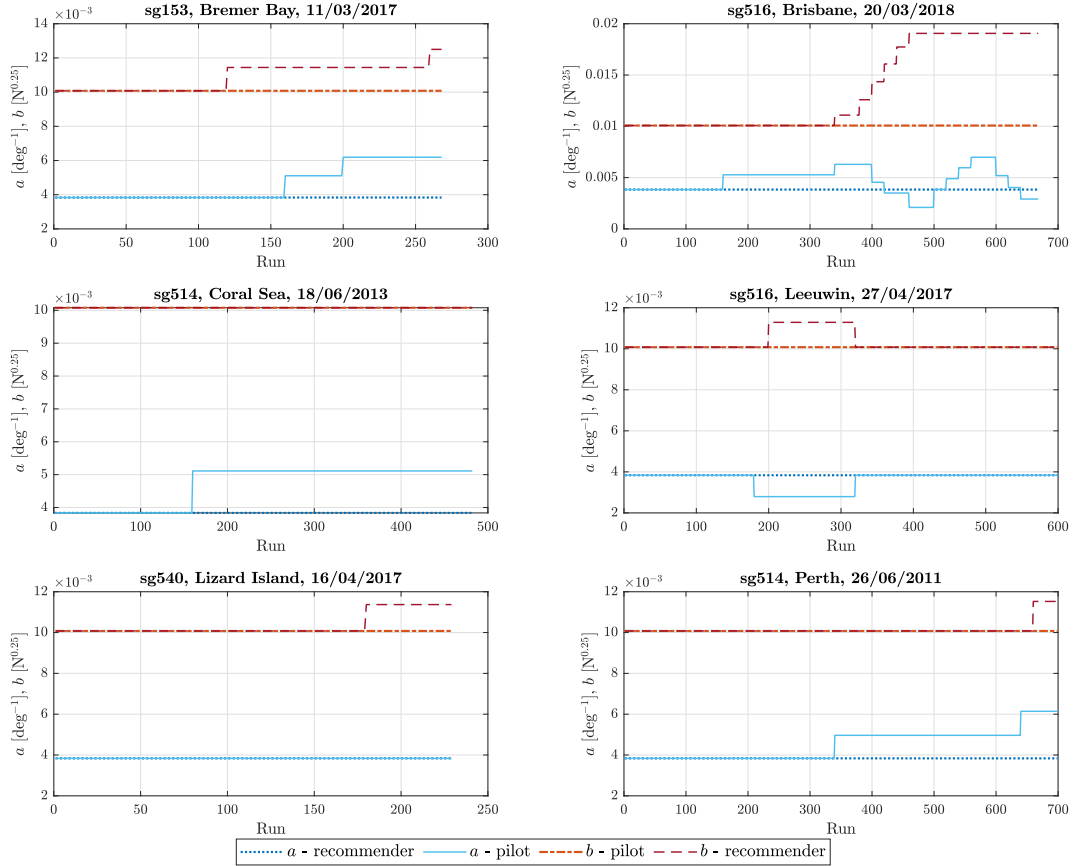


Figure 14: Variation of the lift and drag coefficients with dive profile as selected by the pilots and recommended by the developed system for the missions run by the IMOS.

566 task can be performed in a tank of appropriate size and constant cross-
 567 section filled with seawater, with readings being taken on at least four sides
 568 to average out oscillations (e.g. due to waves). Additionally, from this process
 569 T_0 , i.e. the reference temperature, may be determined. Measuring V_0 before
 570 the deployment would provide higher accuracy than the regression analysis
 571 explained in this article and it would improve the accuracy and computational
 572 speed of the estimation of the hydrodynamic coefficients and compressibility
 573 of the Seaglider by fixing one of the four (or five) flight parameters.

574 The amount of marine growth observed at the end of a deployment should
 575 be quantified and stored in a database so that it may be used to determine
 576 whether tracking the hydrodynamic coefficients may be used for remote con-

577 dition monitoring of the Seaglider.

578 Finally, dive cycles for close to the maximum target depth for the mission
579 should be performed sooner so that the trimming operation may be completed
580 more accurately and faster. However, care needs to be ensured a sufficiently
581 large maximum buoyancy value is allowed at the start so as to ensure the
582 UG will climb to the surface in the worst case scenario before trimming is
583 completed (IRobot, 2012).

584 **5. Conclusions**

585 An effective recommender system for the trim and flight parameters of
586 Seaglidors has been developed to aid trainee pilots and facilitate round-the-
587 clock operations. Although the system presents improvements over standard
588 practices, it relies on the self-same assumption of steady-state flight condi-
589 tions and resulting equations of motion at equilibrium to increase its robust-
590 ness and speed up its implementation. Additionally, suggestions are made
591 for oceanographic centres to reap the benefits from the operation of large
592 fleets of gliders.

593 The performance of the recommender system has been assessed against
594 the selection of the trim and flight parameters of Seaglidors by expert pilots
595 for 12 deployments run by the NOC and IMOS. While the VBD and pitch
596 centres present a very close comparison, greater difference is shown by the
597 roll centres. This is due to removal of the points corresponding to zero roll
598 angle in the recommender system from the linear fit of roll angle with roll
599 control input, since they only contribute to noise. The predicted lift and drag
600 coefficients are also similar to the nominal values, which are selected by the
601 pilots in all analysed deployments. However, for four missions, an increase
602 in drag towards the end of the deployment is likely to be representative of
603 marine growth on the Seaglider. As a result, tracking the hydrodynamic
604 coefficients may be investigated as a tool for the condition monitoring of
605 Seaglidors.

606 The recommender system will now be implemented in the command and
607 control cloud software of the NOC. Due to its high performance, the devel-
608 oped system is expected to greatly help trainee Seaglider pilots achieve a
609 comparable level of expertise to professional pilots from the very beginning.
610 After extensive testing, the system is also anticipated to provide a level of
611 autonomy to gliders' operations during night hours.

612 Acknowledgements

613 The authors would like to thank Stephen Woodward, an expert glider
614 pilot at the NOC, for his help during the collaborative project. C. Harris,
615 A. B. Phillips, and A. Lorenzo Lopez' contributions were funded under the
616 NERC/ISCF Oceanids programme.

617 Appendix A. Determination of the VBD Centre

618 The following further adjustments have been made to reduce the noise in
619 the estimation of the VBD centre:

- 620 • No change is made to C_{vbd} if the dive profile is aborted or if the glider
621 climbs tail up and nose down.
- 622 • An activation function is included so that no change is made if $\delta C_{vbd} <$
623 15 A/D or $\delta C_{vbd} > 999$ A/D, where δC_{vbd} defines the estimated change
624 in VBD centre over the value used as input during the dive.
- 625 • The value of C_{vbd} is averaged over up to 10 past dive profiles or up
626 to as many past dive profiles with the same C_{vbd} as the current one,
627 whichever is smallest. This adjustment is particularly important to
628 filter inaccuracies in the determination of the apogee, e.g. as shown in
629 Figure 3.
- 630 • A further activation is applied so that no change is made unless $\delta C_{vbd} \geq$
631 25 A/D.
- 632 • The value of C_{vbd} is clipped to the maximum and minimum values
633 specified in the manual (iRobot, 2012) so as to prevent the VBD from
634 hitting the end stops.

635 Appendix B. Determination of the Pitch Centre and Gain

636 The following adjustments have been made to reduce the noise in the
637 estimation of the centre and gain of the pitch control mechanism:

- 638 • No change is made if the dive profile is aborted or if the glider climbs
639 tail up and nose down.

- 640 • There is no need to correct for 50% of the expected change in pitch
641 centre and gain, since data from multiple dive profiles is analysed and
642 the absolute value of the pitch centre is determined rather than relative
643 changes.
- 644 • The gain of the pitch control mechanism is not corrected unless the
645 centre is too.
- 646 • The pitch angle and pitch raw control data are accumulated for up
647 to 20 past profiles or up to as many past dive profiles with the same
648 centre of the VBD as the current one, whichever is smallest. Only the
649 data corresponding to an angle of roll $|\phi| < 5^\circ$ is kept to avoid coupled
650 dynamic effects, as identified as a problem by Frajka-Williams et al.
651 (2011). This process is particularly important to smooth out sensor
652 noise.
- 653 • No change is made if $\delta C_\theta < 15$ A/D or $\delta C_\theta > 999$ A/D to remove the
654 effect of numerical errors in the linear fit.
- 655 • The estimate of the pitch gain is filtered over the past 10 values. Fur-
656 thermore, outliers are removed from the pitch gain prediction.
- 657 • The values of the pitch control centre and gain are clipped to the max-
658 imum and minimum values specified in the manual (iRobot, 2012) so
659 as to prevent the battery pack from hitting the end stops.

660 **Appendix C. Determination of the Roll Centres**

661 The following adjustments have been made to reduce noise in the estima-
662 tion of the centres of the roll control mechanism:

- 663 • No change is made if the dive profile is aborted or if the glider climbs
664 tail up and nose down.
- 665 • $C_{\phi,d}$ and $C_{\phi,c}$ are corrected independently of each other.
- 666 • There is no need to correct for 50% of the expected change in roll centre,
667 since data from multiple dive profiles is analysed and the absolute value
668 of the roll centre is determined rather than relative changes.

- 669 • The roll angle and control data are accumulated for up to 20 past
670 profiles or up to as many past dive profiles with the same $C_{\phi,d}$ or $C_{\phi,c}$
671 as the current one, whichever is smallest. This process is particularly
672 important to smooth out sensor noise.
- 673 • No change is made if $\delta C_{\phi} < 15$ A/D or $\delta C_{\phi} > 399$ A/D.
- 674 • The estimate of the roll centre is filtered over the past 10 values. Fur-
675 thermore, a further activation function is applied so that no change is
676 applied unless $\delta C_{\phi} > 49$ A/D to prevent many changes in roll centre,
677 which have found to be a problem in current practice.
- 678 • The values of the roll centres are clipped to the maximum and minimum
679 values specified in the manual (iRobot, 2012) so as to prevent the
680 Seaglider from capsizing.

681 References

- 682 Abbeel, P., Coates, A. and Ng, A. Y. (2010), ‘Autonomous Helicopter Aer-
683 obatics through Apprenticeship Learning’, *The International Journal of*
684 *Robotics Research* **29**(13), 1608–1639.
- 685 Aggarwal, C. C. (2016), *Recommender Systems: The Textbook*, Springer In-
686 ternational Publishing.
- 687 Anderlini, E., Harris, C., Woo, M. and Thomas, G. (2019), A New Recom-
688 mender System for Determining Trim and Flight Parameters of Seaglid-
689 ers, *in* ‘29th International Ocean and Polar Engineering Conference’, ISOPE,
690 Honolulu, HI.
- 691 Bouzekri, E., Canny, A., Fayollas, C., Martinie, C., Palanque, P., Barboni,
692 E., Deleris, Y. and Gris, C. (2017), A list of pre-requisites to make rec-
693 ommender systems deployable in critical context, *in* ‘CEUR Workshop
694 Proceedings’.
- 695 Dao, A. Q. V., Koltai, K., Cals, S. D., Brandt, S. L., Lachter, J., Matessa,
696 M., Smith, D. E., Battiste, V. and Johnson, W. W. (2015), ‘Evaluation of
697 a Recommender System for Single Pilot Operations’, *Procedia Manufac-*
698 *turing* **3**, 3070 – 3077.

- 699 Davis, R., Eriksen, C. and Jones, C. (2003), Autonomous Buoyancy-Driven
700 Underwater Gliders, *in* G. Griffiths, ed., ‘Technology and Applications of
701 Autonomous Underwater Vehicles’, Taylor & Francis, London, pp. 37–52.
- 702 Eriksen, C. C., Osse, T. J., Light, R. D., Wen, T., Lehman, T. W., Sabin,
703 P. L., Ballard, J. W. and Chiodi, A. M. (2001), ‘Seaglider: A Long-
704 Range Autonomous Underwater Vehicle for Oceanographic Research’,
705 *IEEE Journal of Oceanic Engineering* **26**(4), 424–436.
- 706 Frajka-Williams, E., Eriksen, C. C., Rhines, P. B. and Harcourt, R. R. (2011),
707 ‘Determining vertical water velocities from Seaglider’, *Journal of Atmo-
708 spheric and Oceanic Technology* **28**(12), 1641–1656.
- 709 Graver, J. G. (2005), Underwater Gliders: Dynamics, Control and Design,
710 Phd thesis, Princeton University.
- 711 Graver, J. G. and Bachmayer, R. (2003), ‘Underwater glider model parameter
712 identification’, *Proc. 13th Int. Symp.* (August).
- 713 Hussain, N. A. A., Arshad, M. R. and Mohd-Mokhtar, R. (2011), ‘Underwa-
714 ter glider modelling and analysis for net buoyancy, depth and pitch angle
715 control’, *Ocean Engineering* **38**, 1782–1791.
- 716 IRobot (2012), 1KA Seaglider User’s Guide, Technical Report January.
- 717 Kim, G. I., Pham, T. and Rohr, T. C. (2017), ‘US9542851’.
- 718 Leonard, N. E. and Graver, J. G. (2001), ‘Model-based feedback control of
719 autonomous underwater gliders’, *IEEE Journal of Oceanic Engineering*
720 **26**(4), 633–645.
- 721 Li, B. and Su, T. C. (2016), ‘Nonlinear heading control of an autonomous
722 underwater vehicle with internal actuators’, *Ocean Engineering* .
- 723 Mahmoudian, N. and Woolsey, C. (2008), Underwater glider motion control,
724 *in* ‘Proceedings of the IEEE Conference on Decision and Control’.
- 725 Merckelbach, L., Smeed, D. and Griffiths, G. (2010), ‘Vertical water velocities
726 from underwater gliders’, *Journal of Atmospheric and Oceanic Technology*
727 **27**(3), 547–563.

- 728 Osse, T. J. and Eriksen, C. C. (2007), The Deepglider: A Full Ocean
729 Depth Glider for Oceanographic Research, *in* ‘OCEANS’, Vancouver, BC,
730 Canada.
- 731 Queste, B. Y. (2018), ‘The UEA Seaglider Toolbox’.
732 **URL:** <http://www.byqueste.com/toolbox.html>
- 733 Rudnick, D. L. (2016), ‘Ocean Research Enabled by Underwater Gliders’,
734 *Annual Review of Marine Science* **8**(1), 519–541.
- 735 Schofield, O., Kohut, J., Aragon, D., Creed, L., Graver, J., Haldeman, C.,
736 Kerfoot, J., Roarty, H., Jones, C., Webb, D. and Glenn, S. (2007), ‘Slocum
737 Gliders: Robust and ready’, *Journal of Field Robotics* **24**(6), 474–485.
- 738 Stommel, H. (1989), ‘The Slocum Mission’, *Oceanography* **2**(1), 22–25.
- 739 Webb, D. C., Simonetti, P. J. and Jones, C. P. (2001), ‘SLOCUM: An under-
740 water glider propelled by environmental energy’, *IEEE Journal of Oceanic*
741 *Engineering* .
- 742 Williams, C. D., Bachmayer, R. and De Young, B. (2008), Progress in pre-
743 dicting the performance of ocean gliders from at-sea measurements, *in*
744 ‘OCEANS 2008’.
- 745 Wood, S. (2009), Autonomous Underwater Gliders, *in* A. Inzartsev, ed., ‘Un-
746 derwater Vehicles’, IntechOpen, chapter 26, pp. 499–524.
- 747 Zhang, S., Yu, J., Zhang, A. and Zhang, F. (2013), ‘Spiraling motion of
748 underwater gliders: Modeling, analysis, and experimental results’, *Ocean*
749 *Engineering* **60**, 1–13.